ACTA SCIENTIFIC AGRICULTURE (ISSN: 2581-365X)

Volume 2 Issue 10 October 2018

Review Article

Novel Drought Monitoring Model Based on MODIS Image Data

Ai-Di Huo[1,2], Hong Wei[1,2], Yu-xiang Cheng[3], Chun-li Zheng[4], Wen-ke Guan[5]*, Jin-xi Song[6] and Liang Qiao[1]

[1]*School of Environmental Science and Engineering, Chang'an University, Xi'an Shaanxi, China*

[2]*Key Laboratory of Subsurface Hydrology and Ecological Effects in Arid Region, Ministry of Education, Chang'an University, China*

[3]*College of Geology Engineering and Geomatics, Chang'an University, Xi'an Shaanxi, China*

[4]*Department of Environmental Science and Engineering, School of Energy and Power Engineering, Xi'an Jiaotong University, Xi'an, China*

[5]*Afforestation Desert Control Research Institute, Xinjiang Academy of Forestry, Urumqi, China*

[6]*College of Urban and Environmental Sciences, Northwest University, Xi'an, China*

***Corresponding Author:** Wen-ke Guan, Afforestation Desert Control Research Institute, Xinjiang Academy of Forestry, Urumqi, China.

Received: September 04, 2018; **Published:** September 18, 2018

DOI: 10.31080/ASAG.2018.02.0201

Abstract

Droughts are dangerous natural disasters which impact agricultural production and human life across the globe. Remote sensing (RS), geographic information system (GIS) technology and multiple-band composite moderate-resolution imaging spectroradiometer (MODIS) satellite image data were combined to research drought characteristics in Xinjiang Uygur Autonomous Region in this study. A new drought status index (DSI) remote sensing monitoring model was established based on the spectral reflectance properties of water. The model was applied to Xinjiang Uygur Autonomous Region for drought monitoring, and then a spatial distribution map of drought situation grades in Xinjiang was drawn accordingly. Correlation analysis and verification results of the in-situ soil drought status in Tarim River and Gurbantunggut Desert Edge region over the same period were used to establish a drought grade index for RS monitoring. The linear correlation between the model and the measured soil moisture values was significant, suggesting that the model is a good fit for drought monitoring in the Northwest Territories. The model accurately reflects changes in surface moisture, suggesting that it is applicable to a wide range of remote soil drought monitoring methods.

Keywords: Remote Sensing Monitoring; MODIS Image; Soil Moisture; Drought Condition Index; Xinjiang

Introduction

Droughts are the most common natural disaster worldwide. They can cause significant damage to the economy, environment, and society by complicating agricultural practices in the areas in which they occur. Soil moisture is the important factor in any drought monitoring technique; it is the key parameter in climate, hydrology, ecology, and agriculture domains. Soil moisture plays a significant role in matter and energy exchange between the land surface and atmosphere. Traditional methods of drought monitoring capture soil moisture data from meteorological monitoring points, which are limited in quantity and representativeness. Although spatial interpolation can mitigate this disadvantage to some extent, interpolate processing is affected by sample size, spatial distribution, and other limitations which introduce uncertainty [1]. In remote drought sensing monitoring, inversion of soil moisture is very important but highly challenging; soil moisture inversion is affected by temperature, rain, soil type, land cover, and other complex factors. Improved drought monitoring tools are vital for providing decision-makers with accurate and timely information for effective drought planning, mitigation, and response activities.

Remote sensing is dynamic, efficient, rapid, and can encompass a larger scale than traditional methods. It is already often used for drought monitoring at the regional scale. Research on remote sensing technology applications for soil moisture monitoring began in the 1960s. Bowers, for example, established the theoretical foundation of these monitoring techniques: that soil reflectance decreases as bare-soil moisture increases [2]. Watson established

a thermal inertia model using a daily range of land surface temperatures [3]. Rosema [4] improved upon this model for thermal inertia and daily evapotranspiration. Beginning in the 1980s, these techniques began to be extended to ground remote sensing, aviation remote sensing, and satellite remote sensing; the corresponding band range includes visible light, near-infrared, mid-infrared, far-infrared, thermal infrared, and microwave. Qi Shuhua [5] researched Chinese drought states in March and May of 2000 using the Temperature Vegetable Drought Index (TVDI), which combines land surface temperature and plant cover information. An increasing quantity of satellites with microwave sensors has broadened the application of microwaves for soil moisture remote sensing.

Soil water content can be quickly depleted when there is a precipitation deficit, so soil moisture provides direct evidence of areas suffering rain shortages. There currently exist a variety of reliable and feasible methods to measure soil water content from the point scale to the global scale [6]. Among them, soil moisture satellite products offer considerable advantages in terms of global coverage and spatial resolution. They have recently been integrated in several drought monitoring programs [7]. There are two missions currently devoted to global surface soil moisture (SSM, top 0 - 5 cm) monitoring: the Soil Moisture and Ocean Salinity (SMOS) [8] and the Soil Moisture Active and Passive (SMAP) [9]. These two missions provide 40 km global maps of SSM every three days. However, Terra and Aqua are orbiting satellites with local equatorial crossing times of approximately 10:30 P.M./10:30 A.M. for Terra, and 1:30 P.M./1:30 A.M. for Aqua, respectively, in ascending/descending nodes. MODIS products are also freely distributed by the U.S. Land Processes Distributed Active Archive Center (https://lpdaac.usgs.gov) [10]. Only MODIS products were utilized in this study, as they provide higher temporal resolution and spatial resolution than SMAP or SMOS products in the study area.

MODIS is a modern optical remote sensing instrument which combines image with spectral data. It includes 36 spectrum bands ranging from 0.4 μm (visible light) to 14.4 μm (thermal infrared) allowing for very high-quality observations [16]. Thermal inertia facilitates bare-soil drought monitoring, but requires day and night-time data be gathered separately and integrated - this is challenging, especially in cloudy areas. Further, some models have insufficient resolution for soil drought monitoring in desert areas.

The accuracy of climate-based indicators has improved in recent years alongside technological advances. This has improved both the spatial and temporal resolution of the climate data available for drought monitoring. Existing approaches still have generally insufficient spatial precision for monitoring drought patterns, however, because they use discrete, point-based meteorological measurements collected at weather stations. Many studies have capitalized on the synoptic, timely, and spatially continuous characteristics of remotely sensed data gathered by satellites to analyze and monitor vegetation conditions over large areas [13]. The integration of coarser-resolution measured data and higher-resolution, satellite-based vegetation observations provides an alternative approach to monitoring and characterizing the spatial extent, intensity, and local variability of droughts as they affect vegetation conditions.

The primary focus of this paper is a new drought monitoring methodology called the drought status index (DSI), which integrates historical measurement data and satellite-based earth observations with other biophysical information (e.g. land cover, land use, and soil) for mixed areas (e.g. bare-soil and plant). The DSI facilitates drought assessment via a 2 km-resolution indicator of the geographic extent and intensity of drought stress on vegetation. This approach builds on traditional techniques by incorporating new data mining analysis techniques to identify historical climate-vegetation relationships related to drought phenomena. The following discussion highlights the strengths of this index over traditional drought indicators, including the fact that it is applicable over large-scale areas.

Methodology

Relationship between soil drought and spectral reflectance

Satellite remote sensing images are reflections of surface features characterized by electromagnetic waves and their thermal radiation information. Because surface features have different structures and physicochemical properties, their electroreflectance and thermal radiation are different. For water, almost all incident energy (ranging across near-infrared and mid-infrared bands) is absorbed. Conversely, plants and soil absorb little energy in these ranges and instead reflect most of it. These different characteristics make the relationship between soil drought and spectral reflectance clear to the observer.

Figure 1 shows the absorption curve for water in different wavelengths, where peaks occur around 1.4 μm and 2.0 μm. If there is more water in the soil, its reflectance value is lower. Electromagnetic waves near 1.4 μm and 2.0 μm indicate less soil moisture [11]. In MODIS data, the sixth band wavelength is 1.628 μm-1.652 μm, and the seventh band is 2.105 μm - 2.155 μm, which near the

absorption peak of water. MODIS data for these two bands was utilized for soil drought inversion in this study.

Figure 1: Sketches the water absorption curve (Chen and Xiao 1994).

Soil drought model

The drought process is related to the water cycle as a whole including precipitation, soil moisture, vegetation water consumption, and storage in rivers and lakes. Soil moisture is the key factor among them, however, and is generally used to represent the severity of drought.

Soil is a natural complex which includes a variety of components. The soil spectrum is affected by soil parent material, organic matter, water, and other elements; the effect of soil water is particularly significant. As mentioned above, reflectance decreases as soil moisture increases.

MODIS L1B data includes 36 bands. One image covers 2330 5000 km^2 (i.e. covers a large-scale area). Again, the sixth and seventh bands correspond to the water absorption peak; these two bands are sensitive to changes in water reflectance. The sixth band (b_6) is more sensitive than the seventh band (b_7) both to plant and bare-soil reflectance, but both have similar atmospheric scattering and radiation values. The water quantity in plant or soil can be represented by b_6-b_7 values with minimal atmospheric influence. With b6+b7 as the denominator, the result can be limited from -1 to 1.

The proposed DSI model can be expressed as follows:

$$DSI = \frac{b_6 - b_7}{b_6 + b_7} \quad (1)$$

Where, b_6 and b_7 are MODIS reflectance values of the sixth and seventh band, respectively. This model is simple and easily applied, but the re-sample result of 2 km b_6 and b_7 has higher resolution on soil moisture inversion [12,13], so we refined it as follows:

$$DSI = \frac{b_6' - b_7'}{b_6' + b_7'} \quad (2)$$

where b_6'and b_7' are the re-sampling results of b_6, b_7 band at 2 km scale. In most areas of Xinjiang, the reflectance difference of bare land and vegetation is clearly observable, and the former is higher than the latter. To obtain more accurate monitoring results, a plant cover parameter f_v was added to adjust the reflectance difference (b_6'and b_7' bands) for bare soil and plant cover.

Because the reflectance of bare soil is higher than plants in b_6'and b_7' bands, for index uniformity, droughts occurring over plant and bare-soil surfaces can be expressed as follows:

$$DSI_v = f_v DSI \quad (3)$$

$$DSI_S = (1 - f_v) DSI \quad (4)$$

DSI_v and DSI_S are the drought indexes of vegetation canopy and surface-soil, respectively; fv is the vegetation coverage parameter expressed per unit area. The relationship of f_v and NDVI can be expressed as follows [14]:

$$f_v = \frac{NDVI - NDVI_{\min}}{NDVI_{\max} - NDVI_{\min}} \quad (5)$$

$$NDVI = (b_2 - b_1)(b_2 + b_1) \quad (6)$$

$NDVI_{max}$, $NDVI_{min}$ are maximum and minimum NDVI values for the whole growing season over the same period for a multi-year period. (In this paper, $NDVI_{max}$ = 0.818; $NDVI_{min}$ = 0.001.) In Xinjiang, there is more bare land than land with sparse vegetation, so formula (2) can be rewritten as follows:

$$DSI = [1 - 0.817 \times (\frac{b_2 - b_1}{b_2 + b_1})] \times (\frac{b_6' - b_7'}{b_6' + b_7'}) \quad (7)$$

Application and verification of DSI

Xinjiang lies in the mid-latitude hinterland of the Eurasian continent. It is far from the sea, limited in water sources, and features scarce rainfall and strong evaporation typical of arid (and

ecologically fragile) climatic regions. Drought and water shortage are the main environmental characteristics of Xinjiang. Droughts caused by water shortage are the most serious natural disasters that tend to occur in Xinjiang. One-year data (2007, an average year) was used as validation data to analyze drought distribution in this region.

A MODIS image (1 km) from 2007 was chosen as the data source. Homochronous soil moisture data gathered through fieldwork was used to analyze soil drought distribution in the study area; fieldwork is a very important step for model verification.

MODIS is the most important spectroradiometer on Terra, a satellite of the Earth Observation System (EOS). Its data is broadcast across the globe directly. MODIS has three scales of resolution: 250m, 500m and 1000m. The scanning width is 2330 km. The satellite's transit times at the study area are 0:30 and 12:30 (Beijing time). To minimize the influence of cloud cover, we used the 12:30 MODIS image. The MODIS 1B data set was received by the National Meteorological Satellite Center with 1 km resolution as a 16 bit attribute dataset after amendment, adjustment, and enlargement [15,16]. For reflective bands, the result of calibration processing is pixel reflectivity; for thermal infrared bands, the result is pixel radiance.

The ground-based observation time corresponds to MODIS receiving time. Observation areas are located at both sides of Tarim River and the edge of Gurbantunggut Desert in Xinjiang Uygur Autonomous Region. The observation station position and methods we used are similar to those used by Huo and Kang [17].

Study Area

The study area is located between 73°40′- 96°23′E and 34°25′-49°10′N at both sides of the Tarim River and Gurbantunggut Desert in Xinjiang Uygur Autonomous Region. This area is one of the farthest away from the sea in the region. Northern Xinjiang belongs to a temperate continental arid climate zone while Southern Xinjiang belongs to a warm temperate continental arid climate zone. The study area is surrounded on east, south, and north sides by mountains. The area experiences large temperature changes typical of continental arid climates. In recent years, soil drought and land desertification caused by inappropriate land utilization have plagued the area. Figure 2 shows a rough sketch of the study area.

Figure 2: The sketch of land synchronization measuring points distribution.

Results and Analysis

Drought Remote Sensing Monitoring Model

Based on Formula (7), we used the b1, b2, b6, and b7 data from the MODIS image to invert the soil drought status distribution as shown in figure 3. Figure 4 is a scattered diagram between DSI and soil moisture comprised of 81 points detected in July, 2007.

Figure 3 shows that the DSI-based drought status of Xinjiang Uygur Autonomous Region is in accordance with actual measurements, namely, that the most serious drought area was the central portion of the Taklimakan and Gurbantunggut desert areas.

Figure 3: The DSI of Xinjiang Uygur Autonomous Region.

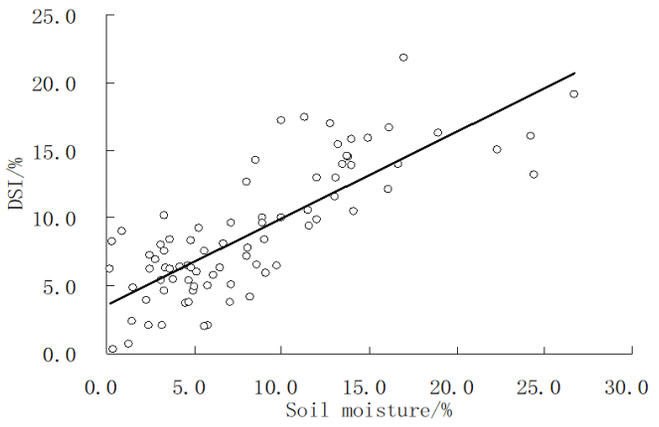

Figure 4: The scattered diagram between DSI and measured soil moisture.

The Takilimakan Desert is located at the center of the Tarim Basin. It is the largest desert in China and tenth largest in the world. Its length is about 1000 km in the east-west direction and its width is about 400 km in the south-northwest direction; its total area is 330,000 km2. The average annual precipitation is below 100 mm, at a minimum as low as 4 - 5 mm, while it's the average evaporation capacity is 2500 - 3400 mm. The Gurbantunggut Desert is located at the center of the Junggar Basin, the second biggest desert in China. The area is 48,800 km2 approximately. These two deserts have the lowest soil moisture across the study area (shaded areas, figure 3). There are several cities scattered throughout these areas including Aksu, Karamay, and Shihezi which have higher soil moisture (light areas, figure 3).

The relativity between DSI and fieldwork values was analyzed by Pearson function as shown in table 1.

Name	Parameters	DSI	Soil moisture
DSI	Pearson R	1	0.793
	Significant probability		0.001
	The number of sample points	81	81
Soil moisture	Pearson R	0.793	1
	Significant probability	0.001	
	The number of sample points	81	81

Table 1: Correlation between soil moisture and DSI using Pearson coefficient.

All relativity values shown in table 1 are higher than 0.79, indicating that the DSI is accurate. We refined the soil moisture model as follows:

All relativity values shown in table 1 are higher than 0.79, indicating that the DSI is accurate. We refined the soil moisture model as follows:

$$M\ (\%) = (0.98 \times DSI - 0.43) \times 100 \quad (8)$$

where, M is modified soil moisture. The variance of the fitting result (R^2) was 0.629 and the average fitting error was 3.73%, so Formula (8) can also be used for the corrected calculation of soil moisture at larger areas.

DSI Grade Standards

Xinjiang's Statistical yearbooks, agricultural statistical yearbooks, drought statistical data, fieldwork data, and remote sensing image data were used to establish the grade standards of DSI shown in table 2. The grading results for the study area are shown in figure 5.

Particularly Severe Drought	0 < DSI ≤ 0.028
Severe Drought	0.028 < DSI ≤ 0.083
Moderate Drought	0.083 < DSI ≤ 0.140
Mild Drought	0.140 < DSI ≤ 0.273
Normal	0.273 < DSI ≤ 0.870

Table 2: Grading index of drought monitoring by remote sensing.

The spatial distribution of drought in Xinjiang province is shown in figure 5. Particularly severe drought occurred at the south side of the Tarim River at where the Takilimakan Desert hinterland is located, its area is around 19.6 km^2. Some particularly severe drought areas were also distributed in the east of Xinjiang. The severe drought grade region was distributed at the north side of Tarim River and Gurbantunggut Desert with a total area around 47 km^2; the moderate drought grade region was located at the central, southern, and eastern edge of Xinjiang. This area was about 48.4 km^2. The mild drought region and normal region was mainly located around larger cities in the region with areas of 29.7 km^2 and 21.2 km^2, respectively.

Cloud cover and differences among statistical methods in various agricultural departments caused some deviation between DSI results and statistical data in regards to specific drought areas.

Overall, however, DSI still yielded reliable reference data for the spatial distribution of droughts across Xinjiang.

Figure 5: The drought magnitude for remote sensing monitoring in Xinjiang Province.

Conclusions

Xinjiang Uygur Autonomous Region was used as a study area to test a new drought monitoring approach combining RS, GIS technology, and multiple-band composite MODIS satellite image data. The spectral reflectance properties of water were used to establish a drought status index-based remote sensing monitoring model. The Xinjiang case study results indicated that DSI indeed reflects dynamic drought phenomena across a large-scale geographical area. Our main conclusions can be summarized as follows:

1) The DSI exploits several MODIS bands and spectral characteristics to yield accurate soil moisture information.
2) DSI data was verified according to the actual drought status of Xinjiang, i.e. fieldwork data gathered in the Tarim River and Gurbantunggut Desert.
3) The calculated area (DSI) of drought regions deviated slightly from the measured areas, but the change trends were the same; to this effect, DSI is a reliable reference for agricultural drought application.

Due to the spatial resolution limitation of MODIS, further research is necessary to successfully fuse other data sources to improve the resolution and quality of the proposed drought remote sensing monitoring technique. There were two important contradictions in this study: the differences in soil moisture depth (only 0 - 20 cm in the fieldwork data, while MODIS reflects only surface information), and differences in collection times (the satellite captures images every few minutes, while fieldwork took place only during the day).

The monitoring technique proposed here may be applicable to vegetation status monitoring, vegetable harvest assessment, hazard assessment, and several other similar domains. The DSI is yet limited by restrictions on the experiment conditions, time, and data in this study. Further studies are necessary to improve the DSI to enhance its applicability to different regions, seasons, and scales.

Acknowledgement

This work was supported by the National Natural Science Foundation of China (Grants No. 41672255, 41877232, 41402255, 41790444 and 41877232); High-tech research cultivation project (Grants No. 300102268202); Program for Key Science and Technology Innovation Team in Shaanxi Province (Grant No. 2014KCT-27), Promoting Higher Education Reform by Big Data Technology, Energizing Future Exploration in Teachers and Students (FPE, Grant No: 2017B00022) and Shaanxi Provincial Institute of Higher Education 2017 Annual Higher Education Research Project (Grant No: XGH17049).

Bibliography

1. Rhee J., *et al*. "Monitoring agricultural drought for arid and humid regions using multi-sensor remote sensing data". *Remote Sensing of Environment* 114.12 (2010): 2875-2887.
2. Bowers S and R Hanks. "Reflection of radiant energy from soils". *Soil Science* 100.2 (1965): 130-138.
3. Watson KM. "The effect of final state interactions on reaction cross sections". *Physical Review* 88.5 (1952): 1163.
4. Rosema A., *et al*. "A new forest light interaction model in support of forest monitoring". *Remote Sensing of Environment* 42.1 (1992): 23-41.
5. Qi S., *et al*. "A national drought monitoring study using temperature vegetation drought index (TVDI)". *Journal of Remote Sensing* 7.5 (2003): 420-427.
6. Martínez-Fernández J., *et al*. "A soil water based index as a suitable agricultural drought indicator". *Journal of Hydrology* 522 (2015): 265-273.

7. Ochsner TE., *et al*. "State of the art in large-scale soil moisture monitoring". *Soil Science Society of America Journal* 77.6 (2013): 1888-1919.

8. Kerr YH., *et al*. "The SMOS mission: New tool for monitoring key elements of the global water cycle". *Proceedings of the IEEE* 98.5 (2010): 666-687.

9. Entekhabi D., *et al*. "The soil moisture active passive (SMAP) mission". *Proceedings of the IEEE* 98.5 (2010): 704-716.

10. Sánchez N., *et al*. "A new Soil Moisture Agricultural Drought Index (SMADI) Integrating MODIS and SMOS Products: a case of study over the iberian Peninsula". *Remote Sensing* 8.4 (2016): 287.

11. Chen W and Q Xiao. "Application of drought monitoring with anomaly vegetation index in 1992". *Environmental Remote Sensing* 9.2 (1994): 106-112.

12. Huo A., *et al*. "Methodology of land surface broadband albedo retrieval in the desertification area based on MODIS image data". In Water Resource and Environmental Protection (ISWREP), 2011 International Symposium: IEEE (2011).

13. Huo A., *et al*. "Assessing the effect of scaling methods on retrieval of soil moisture based on MODIS images in arid regions". *Toxicological and Environmental Chemistry* 98.3-4 (2016): 410-418.

14. Gutman G and A Ignatov. "The derivation of the green vegetation fraction from NOAA/AVHRR data for use in numerical weather prediction models". *International Journal of Remote Sensing* 19.8 (1998): 1533-1543.

15. Huo Ad., *et al*. "Study on remote sensing monitoring model of groundwater level in Aeolian desertification areas-A case study of Mu Us Aeolian desertification areas, China". *Agricultural Research in the Arid Areas* 6 (2010): 37.

16. Huo A., *et al*. "Development and testing of a remote sensing-based model for estimating groundwater levels in aeolian desert areas of China". *Canadian Journal of Soil Science* 91.1 (2011): 29-37.

17. Huo Ad., *et al*. "Simplified Split-window Algorithm Model to Retrieve Land Surface Temperature in Aeolian Desertification Area with MODIS Image Data-Taking North Shaanxi Province as an Example". *Journal of Earth Sciences and Environment* 3 (2009): 016.

Volume 2 Issue 10 October 2018